

Supplementary information for:

**The Counterion ( $\text{SO}_4^{2-}$  and  $\text{NO}_3^-$ ) effect on Crystallographic, Quantum chemical, Protein-, and DNA-binding properties of Two Novel Copper(II)-Pyridoxal-Aminoguanidine complexes**

**Violeta Jevtovic<sup>1,†</sup>, Luka Golubović<sup>2,†</sup>, Odeh A. O. Alshammari<sup>1</sup>, Munirah Sulaiman Alhar<sup>1</sup>, Tahani Y. A. Alanazi<sup>1</sup>, Violeta Rakic<sup>3</sup>, Rakesh Ganguly<sup>4</sup>, Jasmina Dimitrić Marković<sup>2</sup>, Aleksandra Rakić<sup>2</sup> and Dušan Dimić<sup>2,\*</sup>**

<sup>1</sup> Department of Chemistry, College of Science, University of Ha'il, Ha'il 81451, Saudi Arabia; v.jevtovic@uoh.edu.sa (V.J.); odeh.alshammari@uoh.edu.sa (O.A.O.A.); m.alhar@uoh.edu.sa (M.S.A.); ty.alanazi@uoh.edu.sa (T.Y.A.A.)

<sup>2</sup> Faculty of Physical Chemistry, University of Belgrade, Studentski trg 12-16, 11000 Belgrade, Serbia; lukagolubovic3@gmail.com (L.G.); markovich@ffh.bg.ac.rs (J.D.M.); saska@ffh.bg.ac.rs (A.R.)

<sup>3</sup> Toplica Academy of Applied Studies, Department of Agriculture and Food Technology Studies Prokuplje, Ćirila i Metodija 1, 18400 Prokuplje, Serbia; violetachem@gmail.com

<sup>4</sup> Department of Chemistry, Shiv Nadar University, NH-91, Tehsil Dadri, Gautam Buddha Nagar 201314, Uttar Pradesh, India; rakesh.ganguly@snu.edu.in

\* Correspondence: ddimic@ffh.bg.ac.rs

† These authors contributed equally to this work.

**Table S1.** Experimental and theoretical (at B3LYP/6-311++G(d,p)(H,C,N,O)/def2-TZVP(Cu) (Th1) and B3LYP/6-311++G(d,p)(H,C,N,O)/def2-TZVP(Cu) (Th2) level of theory) bond lengths (in Å) of **1**.

Bond	Experimental	Th1	Th2
Cu1-O1	1.8745(17)	1.966	1.958
Cu1-N5	1.915(2)	1.996	1.990
Cu1-O3	1.9418(18)	2.046	2.037
Cu1-N2	1.959(2)	2.013	2.004
Cu1-O9	2.8248(19)	2.310	2.330
O1-C1	1.296(3)	1.284	1.285
N1-C2	1.324(3)	1.339	1.339
N1-C3	1.362(3)	1.362	1.361
C1-C5	1.420(3)	1.431	1.431
C1-C2	1.434(3)	1.430	1.430
O2-C9	1.430(3)	1.413	1.413
N2-C6	1.291(3)	1.291	1.291
N2-N3	1.370(3)	1.356	1.357
C2-C8	1.487(3)	1.488	1.488
N3-C7	1.369(3)	1.365	1.365
C3-C4	1.368(3)	1.373	1.373
O4-N6	1.285(3)	1.269	1.269
N4-C7	1.324(3)	1.353	1.354
C4-C5	1.423(3)	1.419	1.420
C4-C9	1.515(3)	1.523	1.523
O5-N6	1.237(3)	1.218	1.218
N5-C7	1.311(3)	1.310	1.311
C5-C6	1.448(3)	1.445	1.444
O6-N6	1.230(3)	1.284	1.284
O7-N7	1.262(3)	1.277	1.228
N7-O8	1.237(3)	1.228	1.279
N7-O9	1.264(3)	1.269	1.268
R		0.96	0.96
MAE (Å)		0.040	0.04

**Table S2.** Experimental and theoretical (at B3LYP/6-311++G(d,p)(H,C,N,O)/def2-TZVP(Cu) (Th1) and B3LYP/6-311++G(d,p)(H,C,N,O)/def2-TZVP(Cu) (Th2) level of theory) bond angles (in °) of **1**.

Angle	Experimental	Th1	Th2
O1-Cu1-N5	173.83(8)	164.48	165.10
O1-Cu1-O3	91.18(7)	89.11	88.87
N5-Cu1-O3	94.96(8)	101.24	101.09
O1-Cu1-N2	92.16(8)	87.79	88.15
N5-Cu1-N2	81.83(8)	80.13	80.32
O3-Cu1-N2	171.31(8)	170.49	171.02
O1-Cu1-O9	83.44(7)	85.92	85.68
N5-Cu1-O9	96.40(7)	106.20	106.00
O3-Cu1-O9	86.15(7)	85.64	85.28
N2-Cu1-O9	102.20(7)	103.09	102.93
C1-O1-Cu1	127.43(15)	125.39	125.48
C2-N1-C3	124.1(2)	125.04	125.04
O1-C1-C5	127.1(2)	125.87	125.86
O1-C1-C2	115.6(2)	116.70	116.67
C5-C1-C2	117.3(2)	117.43	117.46
C6-N2-N3	119.4(2)	118.83	118.68
C6-N2-Cu1	128.91(17)	129.10	129.15
N3-N2-Cu1	111.71(14)	112.03	112.13
N1-C2-C1	119.7(2)	118.51	118.50
N1-C2-C8	119.3(2)	120.16	120.17
C1-C2-C8	121.0(2)	121.30	121.30
C7-N3-N2	114.97(19)	115.65	115.60
N1-C3-C4	119.7(2)	119.69	119.69
C3-C4-C5	119.5(2)	118.75	118.75
C3-C4-C9	117.7(2)	118.55	118.53
C5-C4-C9	122.8(2)	122.67	122.68
C7-N5-Cu1	114.71(16)	113.21	113.23
C1-C5-C4	119.7(2)	120.53	120.51
C1-C5-C6	121.8(2)	121.34	121.34
C4-C5-C6	118.5(2)	118.12	118.15
O6-N6-O5	122.8(2)	120.67	120.68
O6-N6-O4	119.1(2)	117.19	117.19
O5-N6-O4	118.1(2)	122.13	122.13
N2-C6-C5	122.4(2)	122.87	122.79
O8-N7-O7	120.7(2)	120.06	119.97
O8-N7-O9	120.38(19)	121.20	118.75

O7-N7-O9	118.90(19)	118.74	121.27
N5-C7-N4	126.8(2)	126.98	127.01
N5-C7-N3	116.7(2)	118.16	118.07
N4-C7-N3	116.5(2)	114.83	114.89
N7-O9-Cu1	109.63(14)	116.62	116.39
O2-C9-C4	112.24(19)	111.06	111.08
R		0.99	0.99
MAE [°]		1.77	1.79

**Table S3.** Experimental and theoretical (at B3LYP/6-311++G(d,p)(H,C,N,O)/def2-TZVP(Cu) (Th1) and B3LYP/6-311++G(d,p)(H,C,N,O)/def2-TZVP(Cu) (Th2) level of theory) bond lengths (in Å) of **2**.

Bond	Experimental	Th1	Th2
Cu1-O1	1.886(3)	2.052	2.022
Cu1-N5	1.908(3)	2.000	1.979
Cu1-O3	1.937(4)	2.300	2.348
Cu1-N2	1.974(4)	2.238	2.225
S1-O7	1.448(3)	1.485	1.521
S1-O5	1.467(3)	1.489	1.522
S1-O6	1.471(3)	1.522	1.489
S1-O4	1.495(3)	1.522	1.485
O1-C1	1.304(6)	1.285	1.287
N1-C2	1.333(5)	1.336	1.336
N1-C3	1.365(5)	1.351	1.351
C1-C5	1.421(5)	1.442	1.442
C1-C2	1.421(5)	1.434	1.433
O2-C9	1.432(4)	1.420	1.420
N2-C6	1.277(5)	1.288	1.289
N2-N3	1.369(4)	1.371	1.372
C2-C8	1.490(5)	1.492	1.493
N3-C7	1.369(5)	1.383	1.383
C3-C4	1.369(5)	1.371	1.371
N4-C7	1.344(5)	1.375	1.374
C4-C5	1.418(5)	1.418	1.418
C4-C9	1.514(5)	1.518	1.518
N5-C7	1.301(6)	1.294	1.295
C5-C6	1.454(5)	1.453	1.453
R		0.99	0.98
MAE (Å)		0.049	0.049

**Table S4.** Experimental and theoretical (at B3LYP/6-311++G(d,p)(H,C,N,O)/def2-TZVP(Cu) (Th1) and B3LYP/6-311++G(d,p)(H,C,N,O)/def2-TZVP(Cu) (Th2) level of theory) bond angles (in °) of **2**.

Angle	Experimental	Th1	Th2
O1-Cu1-N5	173.4(2)	159.37	161.10
O1-Cu1-O3	90.01(18)	74.45	74.42
N5-Cu1-O3	96.42(15)	126.14	124.46
O1-Cu1-N2	91.56(18)	83.11	84.30
N5-Cu1-N2	82.00(15)	77.25	77.75
O3-Cu1-N2	178.38(13)	150.70	150.61
O7-S1-O5	109.54(17)	97.34	97.34
O7-S1-O6	111.5(2)	112.03	111.62
O5-S1-O6	110.83(16)	111.83	111.50
O7-S1-O4	108.1(2)	111.49	112.03
O5-S1-O4	108.69(16)	111.76	111.83
O6-S1-O4	108.16(16)	111.62	111.75
C1-O1-Cu1	128.1(4)	132.31	131.48
C2-N1-C3	123.8(3)	124.41	124.39
O1-C1-C5	126.1(4)	125.99	126.12
O1-C1-C2	115.5(4)	117.59	117.39
C5-C1-C2	118.4(3)	116.27	116.35
C6-N2-N3	119.9(3)	117.78	117.85
C6-N2-Cu1	129.3(3)	127.12	125.68
N3-N2-Cu1	110.8(3)	108.31	108.09
N1-C2-C1	119.2(4)	119.47	119.45
N1-C2-C8	119.5(3)	119.24	119.16
C1-C2-C8	121.3(4)	121.28	121.37
N2-N3-C7	115.3(3)	116.64	116.45
N1-C3-C4	119.9(3)	119.70	119.71
C3-C4-C5	119.5(4)	119.44	119.46
C3-C4-C9	118.1(3)	116.36	116.44
C5-C4-C9	122.4(3)	123.55	123.46
C7-N5-Cu1	114.9(3)	117.56	117.49
C4-C5-C1	119.2(3)	119.69	119.64
C4-C5-C6	118.4(3)	117.53	117.54
C1-C5-C6	122.4(3)	122.37	122.36
N2-C6-C5	122.5(4)	123.40	123.16
N5-C7-N4	126.9(4)	126.37	126.36
N5-C7-N3	117.0(3)	120.14	120.04
N4-C7-N3	116.1(4)	113.46	113.56

O2-C9-C4	112.8(3)	110.60	110.55
R		0.88	0.89
MAE [°]		4.28	4.13

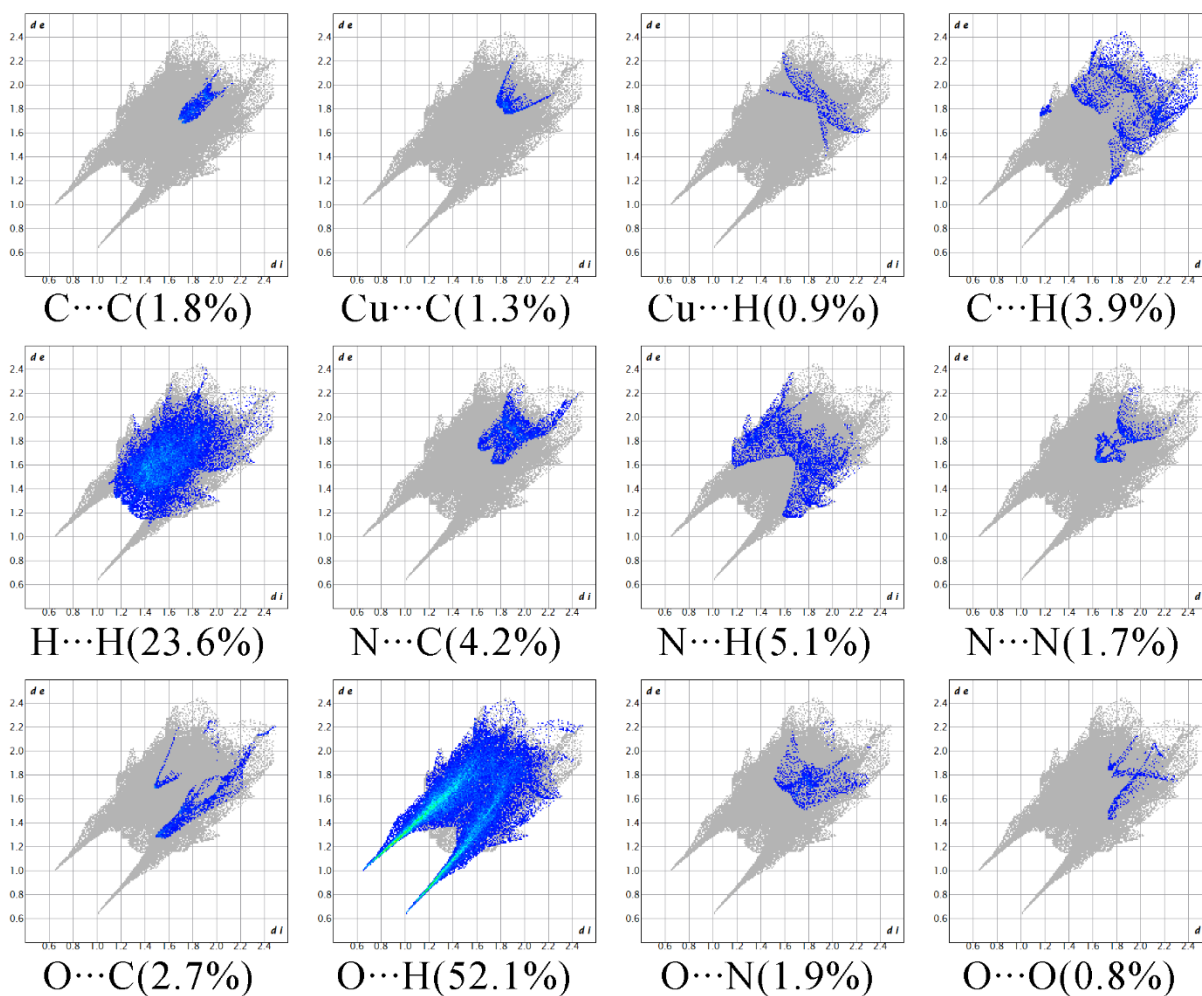


**Figure S1.** The most numerous contacts within the crystal structure of **1**.

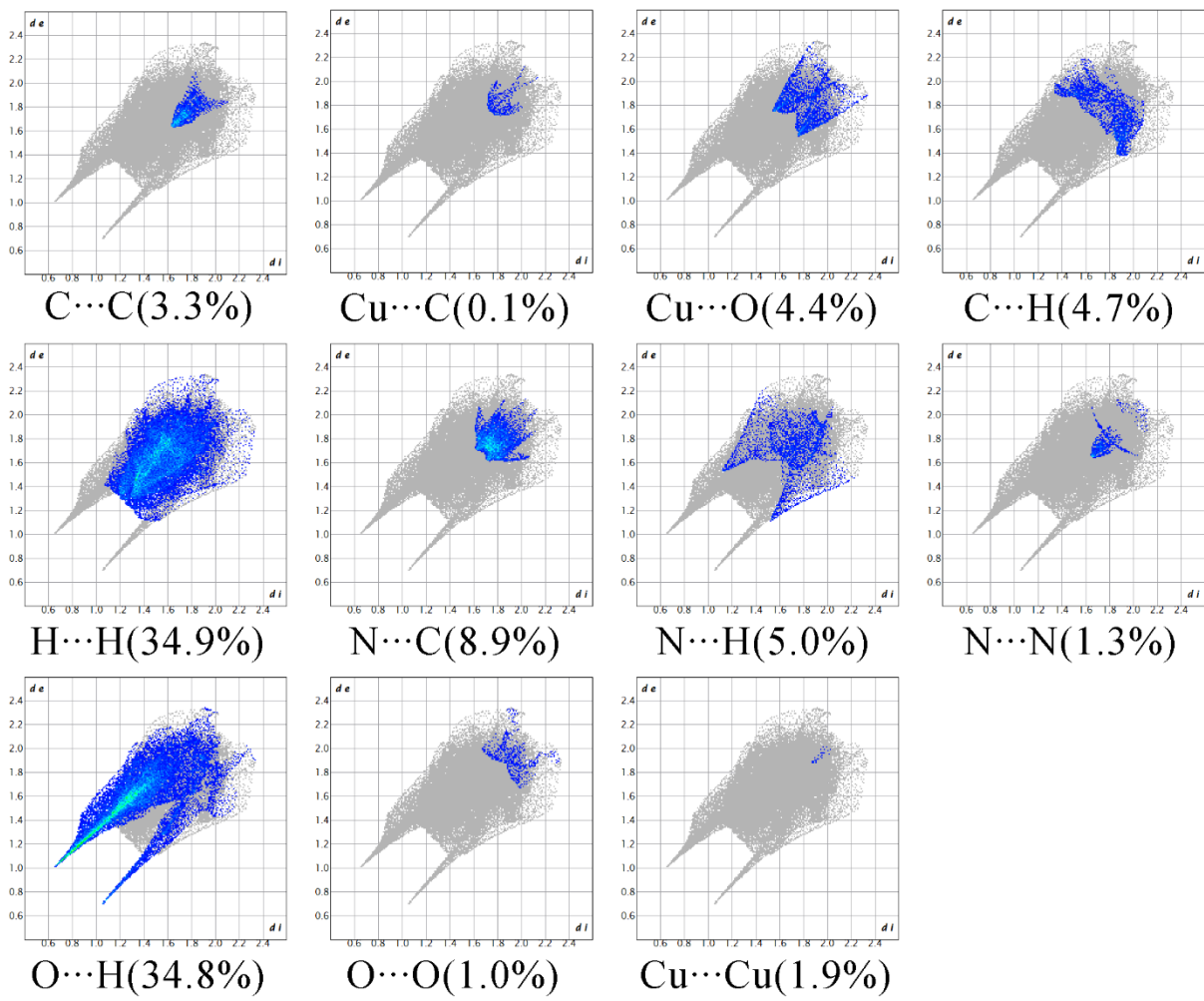


**Figure S2.** The most numerous contacts within the crystal structure of **2**.

**Table S5.** The calculated Bond Critical Points (BCP) properties at the DFT/B3LYP-D3BJ/6-311+G(d,p)/def2-TZVP level of theory: the electron density ( $\rho(r)$ ) and its Laplacian ( $\nabla^2\rho(r)$ ); the Lagrangian kinetic electron density ( $G(r)$ ) and the potential electron density ( $V(r)$ ); the density of the total energy of electrons ( $H(r)$ ) – Cremer-Kraka electronic energy density; the interatomic bond energy,  $E_{\text{bond}}$ . (these interactions are depicted in the following figure)

Bond	$\rho(r)$ [a.u.]	$\nabla^2\rho(r)$ [a.u.]	$G(r)$ [kJ mol <sup>-1</sup> ]	$V(r)$ [kJ mol <sup>-1</sup> ]	$H(r)$ [kJ mol <sup>-1</sup> ]	$-G(r)/V(r)$	$E_{\text{bond}}$ [kJ mol <sup>-1</sup> ]
<b>Complex 1</b>							
Cu1-O1 (1)	0.076	0.516	336.1	-333.4	2.6	1.01	-166.7
Cu1-O3 (2)	0.063	0.422	262.6	-249.4	13.1	1.05	-124.7
Cu1-N2 (3)	0.079	0.443	307.2	-336.1	-28.9	0.91	-168.0
Cu1-N5 (4)	0.082	0.442	312.4	-333.4	-21.0	0.94	-166.7
Cu1-O9 (5)	0.035	0.185	107.6	-94.5	13.1	1.14	-47.3
O3-H...O8 (6)	0.064	0.148	136.5	-173.3	-36.8	0.79	-86.6
C8-H...O8 (7)	0.006	0.020	10.5	-10.0	0.5	1.05	-5.0
C8-H...O7 (8)	0.006	0.020	10.5	-10.2	0.3	1.03	-5.1
O2-H...O4 (9)	0.024	0.0997	60.4	-54.1	6.3	1.12	-27.0
C3-H...O4 (10)	0.021	0.072	42.0	-35.7	6.3	1.18	-17.9
N3-H...O6 (11)	0.060	0.143	126.0	-155.7	-29.7	0.81	-77.8
N4-H...O6 (12)	0.011	0.045	23.6	-19.2	4.5	1.23	-9.6
<b>Complex 2</b>							
Cu1-O1 (1)	0.061	0.434	267.8	-252.0	15.8	1.06	-126.0
Cu1-O3 (2)	0.035	0.195	115.5	-102.4	13.1	1.13	-51.2
Cu1-N2 (3)	0.048	0.249	154.9	-147.0	7.9	1.05	-73.5
Cu1-N5 (4)	0.080	0.476	328.2	-346.6	-18.4	0.95	-173.3
O2-H...O4 (5)	0.021	0.083	47.3	-42.0	5.2	1.12	-21.0
N1-H...O5 (6)	0.025	0.095	55.1	-49.9	5.2	1.11	-24.9
O3-H...O1 (7)	0.025	0.107	63.0	-57.7	5.2	1.09	-28.8
C3-H...O5 (8)	0.012	0.043	23.6	-21.0	2.6	1.12	-10.5

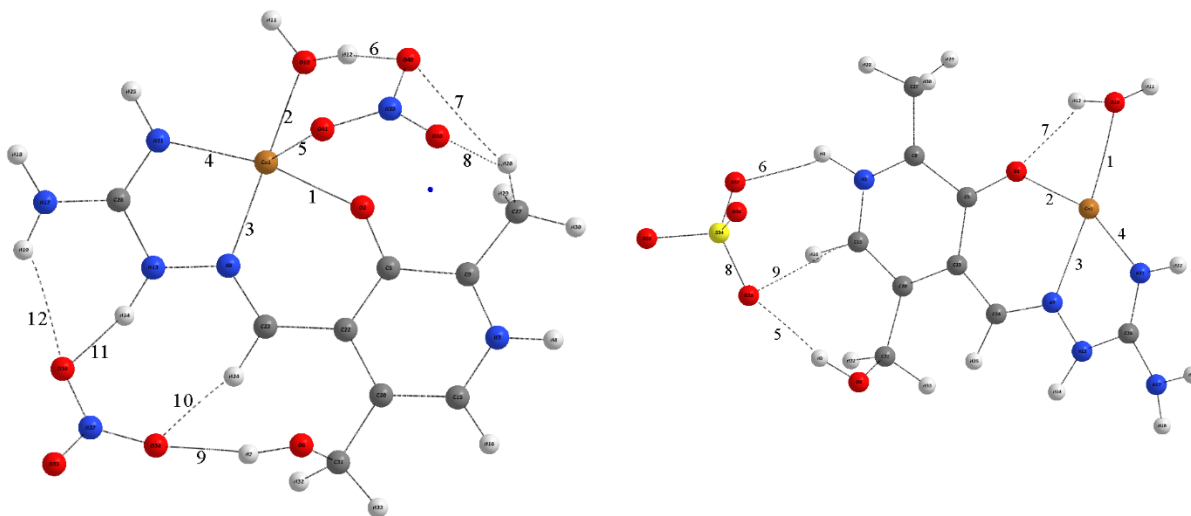


**Figure S3.** The most important Bond Critical Points within optimized structures of Complex 1 (left) and Complex 2 (right).

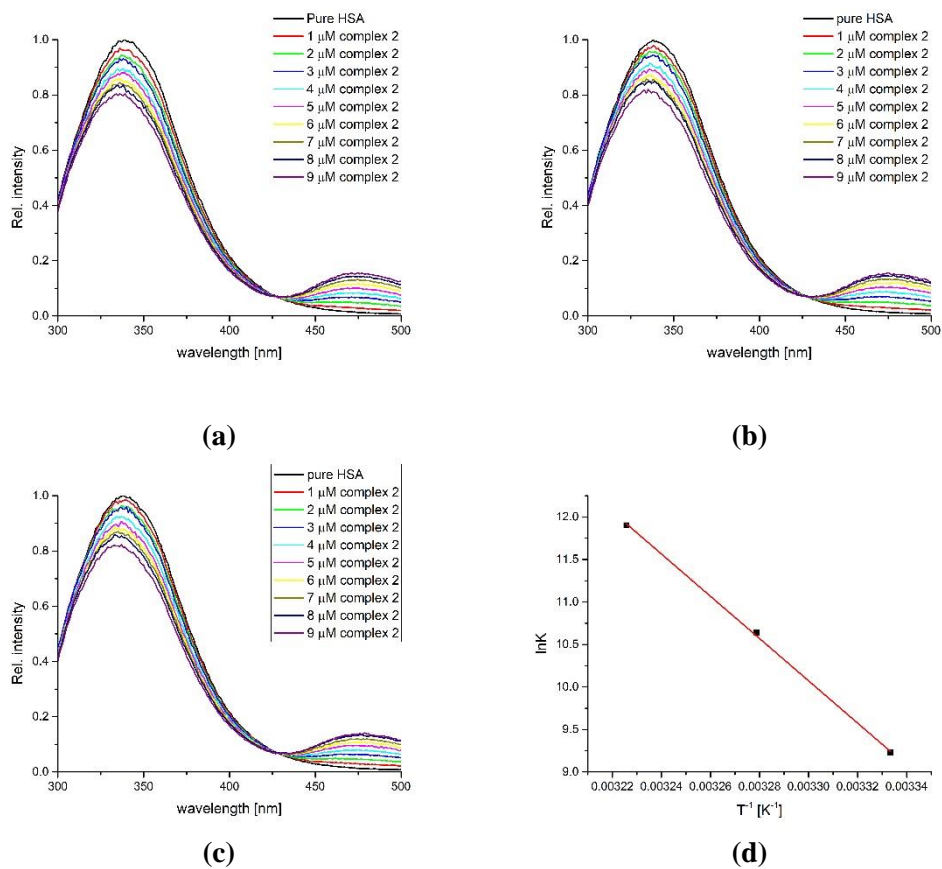


**Figure S4.** Fluorescence emission spectra of HSA for the titration with complex 2 at (a) 27°, (b) 32°, (c) 37°C, and (d) van't Hoff plot for the binding process

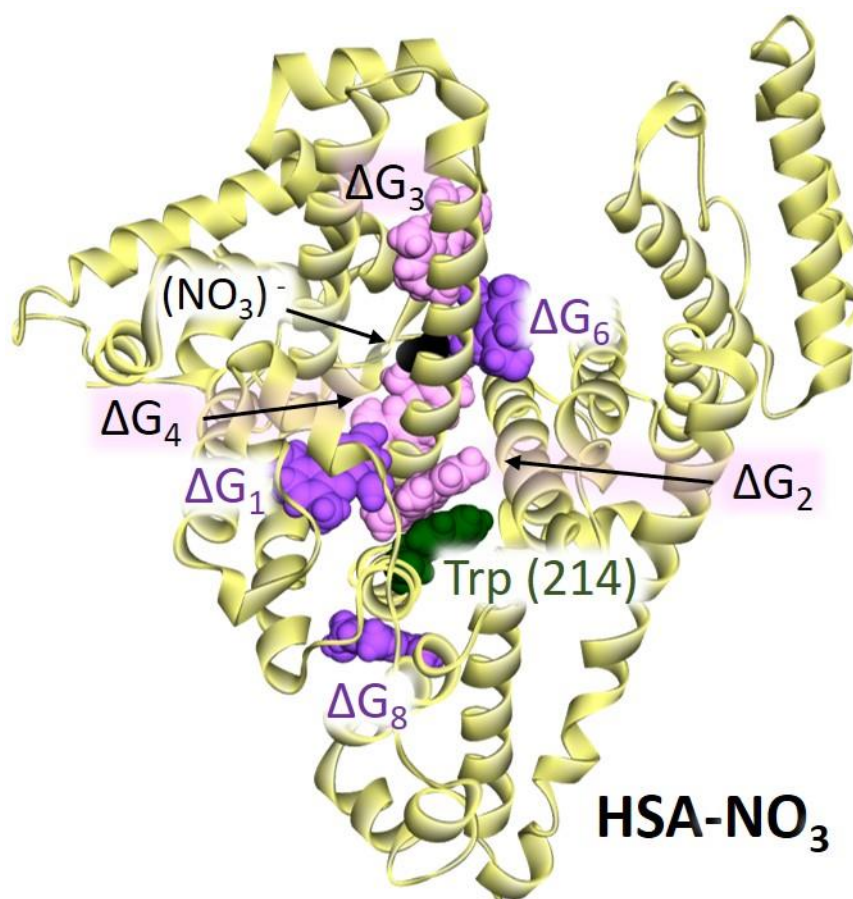


**Figure S5.** Binding positions of Cu-PLAG within the best adduct between HSA (PDB ID: 1S4L) and sulfate anion. Binding positions are denoted by the corresponding index number of the Gibbs free binding energies:  $\Delta G_1$  (Conformation 1),  $\Delta G_2$  (Conformation 2, 9),  $\Delta G_3$  (Conformations 3),  $\Delta G_4$  (Conformations 4, 5, 7, 10),  $\Delta G_6$  (Conformation 6), and  $\Delta G_8$  (Conformation 8). The highest binding energy value is denoted by the lowest index (1), while the lowest value is denoted by the index 8. For clarity, only the orientation of Cu-PLAG with the highest energy value is shown at each binding position, with others omitted. Data for all binding orientations of Cu-PLAG to HSA can be found in Table S7. Cu-PLAG molecules, sulfate ion, and Trp214 residue are depicted in ball representation. Sulfate ions are colored black, Trp214 residue is dark green, while Cu-PLAG molecules are violet and pink in their binding position. The Cu-PLAG molecules are in close proximity. Without introducing subtle color differences, these binding positions would visually merge.

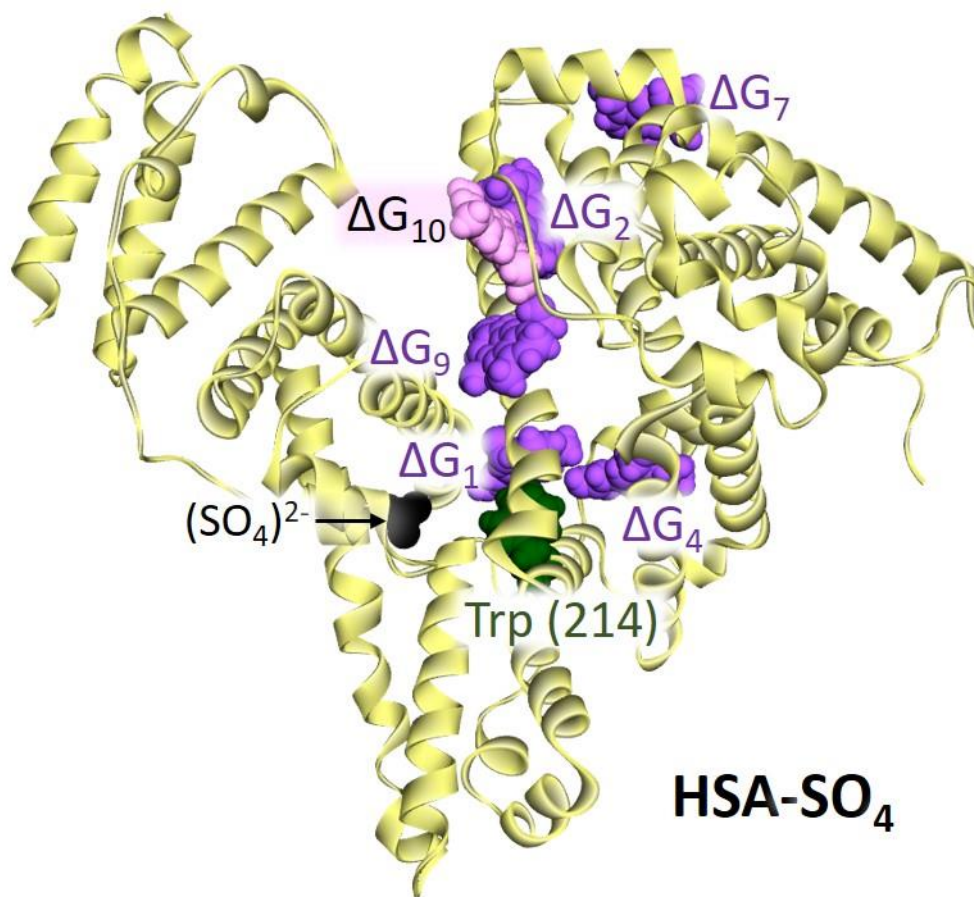


**Figure S6.** Binding positions of Cu-PLAG within the best adduct between HSA (PDB ID: 7WLF) and sulfate anion. Binding positions are denoted by the corresponding index number of the Gibbs free binding energies:  $\Delta G_1$  (Conformation 1),  $\Delta G_2$  (Conformation 2, 3),  $\Delta G_4$  (Conformations 4,5,6,8)  $\Delta G_7$  (Conformation 7),  $\Delta G_9$  (Conformation 9), and  $\Delta G_{10}$  (Conformation 10). The highest binding energy value is denoted by the lowest index (1), while the lowest value is denoted by the index 10. For clarity, only the orientation of Cu-PLAG with the highest energy value is shown at each binding position, with others omitted. Data for all binding orientations of Cu-PLAG to HSA can be found in Table S7. Cu-PLAG molecules, sulfate ion, and Trp214 residue are depicted in ball representation. Sulfate ions are colored black, Trp214 residue is dark green, and Cu-PLAG molecules are violet in their binding position. Additionally, Cu-PLAG in binding position  $\Delta G_{10}$  is colored pink for clarity. The Cu-PLAG molecules in binding positions  $\Delta G_2$ ,  $\Delta G_9$ , and  $\Delta G_{10}$  are in close proximity. Without introducing subtle color differences, these binding positions would visually merge.

**Table S6.** Data for every binding conformation of Cu-PLAG in HSA structures (PDB ID: 6R7S and 1WLF) are listed, including  $\Delta G$  – change in Gibbs free energy of binding, the position of the binding site, and the subdomain to which it belongs.

HSA target (ion)	Cu-PLAG conformation No.	$\Delta G$ (kJ/mol)	Position	Subdomain
6R7S ( $\text{NO}_3^-$ )	1	-29.7	FA7	IIA, near Trp(213)
	2	-29.3	FA8	near Trp(213)
	3	-28.0	FA1	IB
	4	-27.6	between IIA, IIB, and IIIA	
	5	-26.4	between IIA, IIB, and IIIA	
	6	-25.9	outside	IB
	7	-25.5	between IIA, IIB, and IIIA	
	8	-25.5	between IIA and IIB	
	9	-25.5	FA8	near Trp(213)
	10	-25.1	between IIA, IIB, and IIIA	
1WLF ( $\text{SO}_4^{2-}$ )	1	-27.6	FA8	near Trp(213)
	2	-27.2	FA1	IB
	3	-27.2	FA1	IB
	4	-26.4	FA7	IIA, near Trp(213)
	5	-25.5	FA7	IIA, near Trp(213)
	6	-25.5	FA7	IIA, near Trp(213)
	7	-25.1	outside	IB
	8	-25.1	FA7	IIA, near Trp(213)
	9	-24.7	outside	IB
	10	-24.7	outside	IB

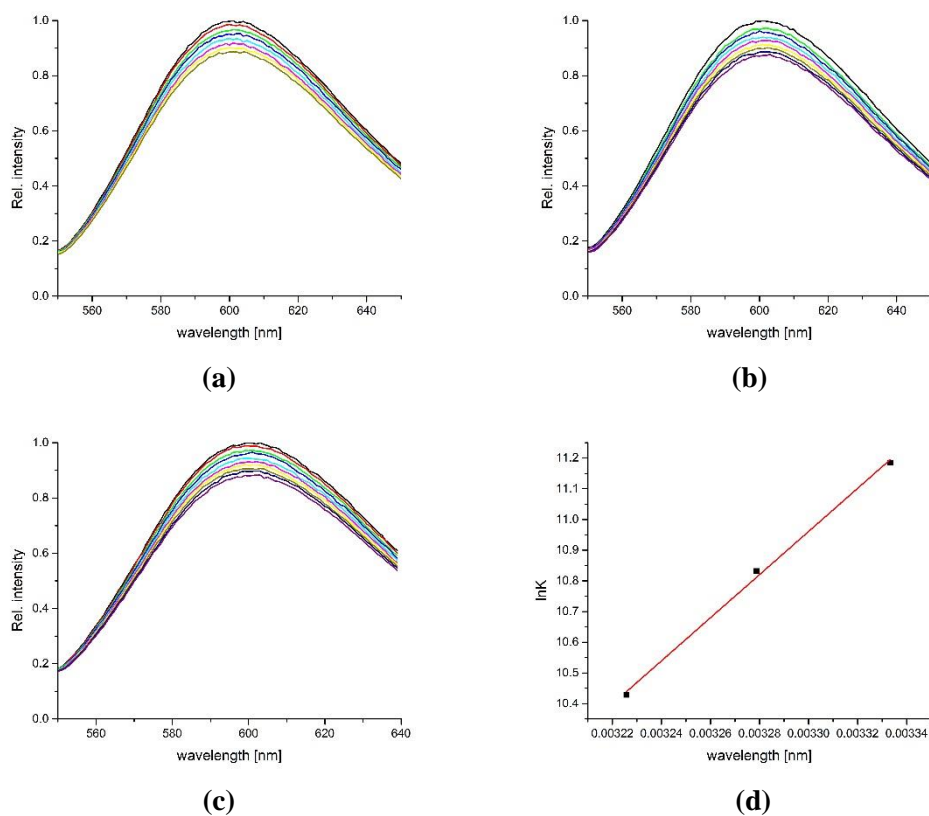


**Figure S7.** Fluorescence emission spectra of DNA for the titration with complex **2** at (a) 27°, (b) 32°, (c) 37°C, and (d) van't Hoff plot for the binding process. (lines: black-pure DNA-EB and with added complex **1**: green – 1 μM, green – 2 μM, blue – 3 μM, magenta – 4 μM, cyan – 5 μM, yellow – 6 μM, dark yellow – 7 μM, navy – 8 μM, and purple – 9 μM)

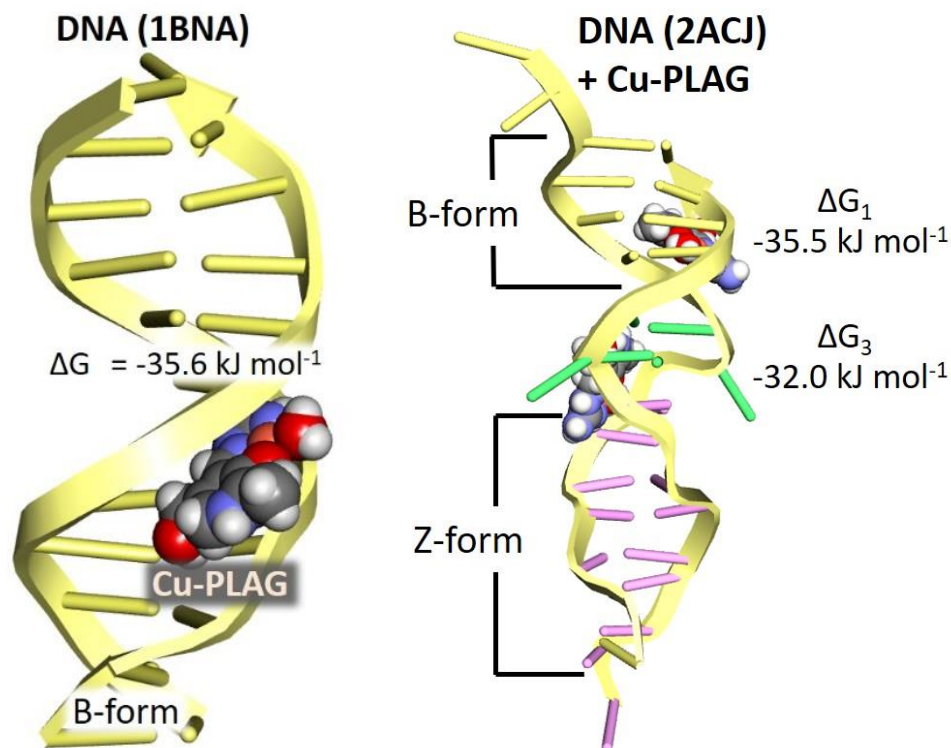


**Figure S8.** Cu(II) complex (Cu-PLAG) adducts with (left) DNA in B-form (PDB ID: 1BNA) and (right) DNA structure (PDB ID: 2ACJ), including both B-form (yellow sticks) and Z-form (pink sticks). The green sticks represent the transition region between two DNA forms. The Cu(II) complex molecules (Cu-PLAG) are depicted in ball representation, with each element colored differently.  $\Delta G$ ,  $\Delta G_1$ , and  $\Delta G_3$  values represent the change in Gibbs free energy of binding of Cu-PLAG to DNA at their binding sites. For clarity, only the orientation of Cu-PLAG with the highest energy value is shown at each binding position, with others omitted. Data for all binding orientations of Cu-PLAG to HSA can be found in Table S7. One binding site in the 1BNA structure accommodates all three binding sites. The  $\Delta G_1$  binding site contains conformations 1 and 2, while the  $\Delta G_3$  binding site accommodates conformations 3 and 4 of the Cu-PLAG molecule in the 2ACJ structure of the DNA molecule. Data for all binding orientations of Cu-PLAG to DNA can be found in Table S7.

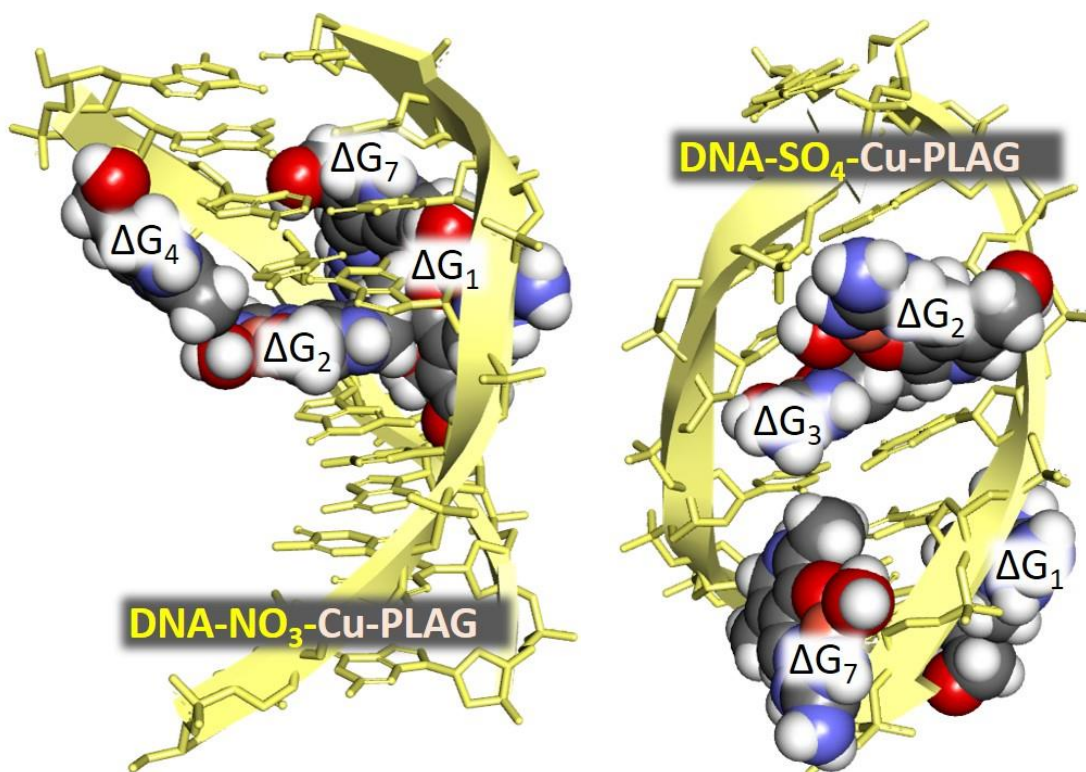


**Figure S9.** Adducts of Cu(II) complex (Cu-PLAG) and DNA (PDN ID: 1XRW) in the presence of (left) nitrate ions (right) sulphate ions. The DNA structure is colored yellow, and Cu-PLAG molecules in their binding positions are depicted in ball representation, colored according to the element type. Counterions are omitted for clarity. Binding positions are denoted by the corresponding index number of the Gibbs free binding energies. In the presence of nitrate ions, the binding positions are  $\Delta G_1$  (Conformation 1),  $\Delta G_2$  (Conformation 2,3,5,6),  $\Delta G_4$  (Conformations 4), and  $\Delta G_7$  (Conformation 7). In the presence of sulfate ions, the distribution of binding positions inside the DNA molecule changes to  $\Delta G_1$  (Conformation 1),  $\Delta G_2$ , (Conformation 2),  $\Delta G_4$  (Conformations 3,4,5,6), and  $\Delta G_7$  (Conformation 7). The highest binding energy value is denoted by the lowest index (1), while the lowest value is denoted by the index 7. For clarity, only the orientation of Cu-PLAG with the highest energy value is shown at each binding position, with others omitted. Data for all binding orientations of Cu-PLAG to DNA can be found in Table S7.

**Table S7.** Data for every binding conformation of Cu-PLAG in DNA structures (PDB ID: 1BNA, 1XRW, and 1ACJ) are listed, including  $\Delta G$  – change in Gibbs free energy of binding and position of the binding site.

DNA target (ion)	Cu-PLAG conformation No.	$\Delta G$ (kJ/mol)	Position
1BNA	1	-35.6	Minor groove
	2	-35.0	
	3	-33.6	
1XRW (NO <sub>3</sub> ) <sup>-</sup>	1	-27.2	Intercalation site from the minor groove side
	2	-26.6	Intercalation site from the major groove side
	3	-26.2	Major groove
	4	-26.0	
	5	-25.8	Intercalation site from the major groove side
	6	-25.0	Minor groove
	7	-24.6	
1XRW (SO <sub>4</sub> ) <sup>2-</sup>	1	-27.3	Major groove
	2	-26.2	Intercalation site from the minor groove side
	3	-26.1	Intercalation site from the major groove side
	4	-25.8	
	5	-25.8	
	6	-25.5	
	7	-24.7	Minor groove
2ACJ	1	-35.5	Minor groove
	2	-33.6	
	3	-32.0	Transition region
	4	-30.8	